

1 Island size shapes genomic diversity in a great speciator (Aves: *Zosterops*)

2 Ethan F. Gyllenhaal^{1*}, Michael J. Andersen², Robert G. Moyle³, Joseph D. Manthey^{1*}

3 ¹Department of Biological Sciences, Texas Tech University, Lubbock, TX, USA

4 ² Department of Biology and Museum of Southwestern Biology, University of New Mexico,
5 Albuquerque, NM 87111

6 ³Department of Ecology and Evolutionary Biology and Biodiversity Institute, University of
7 Kansas, Lawrence, KS 66045

8 *Corresponding author

9

10 **Abstract.**

11 Islands have long represented natural laboratories for studying many aspects of ecology and
12 evolutionary biology, from speciation to community assembly. One aspect that has been well
13 documented is the correlation between island size and taxonomic diversity, likely due to
14 decreased complexity and population size on small islands. This same logic can apply to genetic
15 diversity, which should predictably decrease with effective population size. The island size-
16 diversity correlation has received support over the years, but often focuses on single metrics of
17 genetic diversity. Here, we use *Zosterops* white-eyes in the Solomon Islands to study the
18 correlation between island size and various metrics related to genetic diversity, including runs of
19 homozygosity and fixation of transposable elements. We find that almost all these metrics
20 strongly correlate with island size, and in turn with each other. We infer that island size is
21 independently correlated with these different variables, demonstrating that population size

22 impacts genomic metrics of diversity in a variety of ways across temporal and hierarchical
23 scales.

24

25 **Introduction.**

26 Genetic diversity is the fundamental component of adaptation and persistence, and
27 understanding how variation is distributed among populations is essential for understanding how
28 natural populations evolve (Wright 1982; Hughes et al. 2008). Islands serve as natural
29 laboratories for exploring diverse topics in ecology and evolutionary biology, such as speciation
30 and community assembly, because of their discrete geographic boundaries (Mayr 1942;
31 MacArthur and Wilson 1967; Whittaker et al. 2017). Although archipelagos are characterized by
32 dynamism, island size can be used as a proxy for population size, particularly in population
33 genetic timescales in more stable archipelagos such as those produced by subduction zones
34 (Neall and Trewick 2008). The fact that many species effectively occupy the whole island also
35 allows robust modeling of species ranges over time with bathymetric data and data on sea level
36 change (Tan et al. 2023). Thus, oceanic islands are useful as reliable proxies for estimating
37 population size over time, which is a key factor influencing genetic diversity (Soulé 1976;
38 Frankham 1996).

39 The species-area relationship (Preston 1962a, 1962b) and island biogeographic theory
40 (MacArthur and Wilson 1963, 1967) suggest that larger islands host greater species richness,
41 often due to increased habitat complexity and population sizes. Island biogeographic theory also
42 postulates that distance between regions, a proxy for connectivity, correlates with species
43 richness. The same stochastic processes that operate on taxonomic diversity should shape genetic
44 diversity. This relationship between island size and genetic diversity has been observed in

45 numerous taxa and geographic contexts, such as lizards (Soulé and Yang 1973, Gorman et al.
46 1975), rodents (Patton 1984; Sato et al. 2017), frogs (Wang et al. 2014), and birds (Hoeck et al.
47 2010; Manthey et al. 2020). Such patterns have also been documented in continental contexts,
48 including "sky islands" (Hill et al. 2017; Costanzi and Steifetten 2019) and habitat patches
49 (Descimon and Napolitano 1993). Many of these studies focused on a single measures of genetic
50 diversity and few included complex but important genomic metrics, such as those relevant to
51 demographic history (e.g., effective population size over time) and conservation genetic health
52 (e.g., runs of homozygosity; Szpiech et al. 2013; Ceballos et al. 2018) .

53 *Zosterops* white-eyes, a species-rich bird radiation across the Afro- and Australasian
54 tropics, present an ideal system for studying these patterns. Distributed across many Indo-Pacific
55 islands, they have long been central to speciation theory (e.g., Mayr 1942) and discussions of the
56 'great speciator' paradox (Diamond et al. 1976). Past work has also demonstrated high
57 population densities, even in range-restricted endemics (Cowles et al. 2021). Rapid
58 diversification within *Zosterops* has also made relationships within this clade difficult to resolve
59 (Moyle et al. 2009; Cai et al. 2018; Oliveros et al. 2021, Vinciguerra et al. 2023). The *Zosterops*
60 *griseotinctus* complex is largely composed of phenotypically distinct yet genetically similar
61 endemics in the Solomon Islands and exhibits intricate patterns of gene flow (Manthey et al.
62 2020).

63 In this study, we used whole-genome resequencing of 15 species from the *Z.*
64 *griseotinctus* complex to test the hypothesis that genomic diversity and other metrics of genetic
65 variation correlate predictably with island size. We hypothesize a positive correlation between
66 island size and (1) effective population size, (2) genome-wide genetic diversity, and (3) the
67 variability of genetic diversity across the genome. Conversely, we predict a negative correlation

68 between island size and the length and number of runs of homozygosity. Finally, we expect to
69 see fixation of derived polymorphic transposable elements (TEs) in smaller island populations,
70 as these generally slightly deleterious elements are more readily selected against in large
71 populations (Jurka et al. 2011, Leroy et al. 2021).

72

73 **Methods.**

74 **Reference genome editing and TE annotation.** We used the *Zosterops lateralis* genome
75 (Cornetti et al. 2015) as a reference for this work. Because this genome was highly fragmented,
76 we used Satsuma v2 (Grabherr et al. 2010) and the *Taeniopygia guttata* chromosome-scale
77 genome assembly (Warren et al. 2010) to assign chromosomal coordinates to the *Z. lateralis*
78 genome.

79 We annotated TEs and repetitive elements in the *Z. lateralis* genome using
80 RepeatModeler v1.0.11 (Smit and Hubley 2008) followed by manual TE curation.
81 RepeatModeler uses multiple programs to identify repeats: RECON (Bao and Eddy 2002),
82 RepeatScout (Price et al. 2005), and Tandem Repeats Finder (Benson 1999). We filtered
83 sequences previously curated ($\geq 98\%$ identity) in the RepBase vertebrate database v24.03 (Jurka
84 et al. 2005) and created consensus sequences of novel elements with manual curation. We
85 refined RepeatModeler consensus sequences as follows: (1) extract sequences matching *de novo*
86 repetitive elements and flanking sequence with BLAST and bedtools (Camacho et al. 2009;
87 Quinlan and Hall 2010), (2) alignment of extracted sequences using MAFFT (Kato and
88 Standley 2013), (3) trim ambiguous nucleotides on edges of newly created consensus sequences,
89 and (4) repeating up to two times for any consensus sequences without recovered edges. We
90 assessed any similarity of *de novo* elements to previously curated RepBase sequences with

91 BLAST, using matches for naming purposes. Lastly, we used the RepBase vertebrate database
92 and newly curated repeats with RepeatMasker v4.08 (Smit et al. 2015) to mask and summarize
93 repetitive and transposable elements in the *Z. lateralis* genome.

94 **Resequencing and genotyping.** We used a total of 17 *Zosterops* individuals in this study
95 (Table S1), including 15 from the Solomon Islands (Fig. 1A), the closely related *Z. griseotinctus*,
96 and outgroup *Z. simplex*. The Solomon Islands samples represented 9 species and 11 subspecies,
97 with a single sample per island, excluding two sympatric species on Kolombangara (Table S1).
98 Although the sample size per island was low, the metrics we chose were designed for single
99 samples of similarly high depths of coverage (Fig. S1), as should be representative of the
100 population. We used DNA extractions from previous work in these taxa (e.g., Manthey et al.
101 2020) to create Illumina sequencing libraries, and sequenced on a NovaSeq6000 at the Oklahoma
102 Medical Research Foundation (OMRF) Clinical Genomics Center. We aimed to sequence each
103 individual at 10–20x genomic coverage, and most samples reached this expectation (Fig. S1).

104 We used the bmap (Bushnell 2014) script bbduk.sh to trim sequencing adapters and
105 quality filter raw sequencing data. We aligned reads to the reference genome using the BWA-
106 MEM function in BWA (Li and Durbin 2009) and samtools v1.4.1 (Li et al. 2009) to convert the
107 output to BAM format and measure sequencing depth (Fig. S1). We cleaned, sorted, added read
108 groups to, and removed duplicates from each BAM file using the Genome Analysis Toolkit
109 (GATK) v4.1.0.0 (McKenna et al. 2010). We genotyped all individuals using three steps in
110 GATK: (1) HaplotypeCaller function to call genotypes per individual, (2) CombineGVCFs
111 function to concatenate output, and (3) GenotypeGVCFs to group genotype all individuals for
112 variant and invariant sites. We used VCFtools v0.1.14 (Danecek et al. 2011) to filter output
113 genotyped sites to: (1) minimum site quality of 20, (2) minimum genotype quality of 20, (3)

114 minimum depth of coverage of 5, and (4) maximum mean depth of coverage of 30. Some
115 analyses used additional restrictions on data quality (see appropriate methods sections).

116 ***Phylogenomics.*** We estimated phylogenies for non-overlapping 25 kbp sliding windows
117 using RAxML v8.2.12 (Stamatakis 2014) with the GTRGAMMA model of sequence evolution,
118 the most flexible model available, which allows variable substitution rates and is time-reversible.
119 Here, we filtered our data to include only biallelic and invariant sites and required a minimum of
120 10,000 genotyped sites to retain the window, resulting in 40,257 windows retained. From these
121 40,257 phylogenies, we estimated a species tree using two methods: (1) maximum clade
122 credibility tree of all input trees using DendroPy to determine which input tree is best supported
123 by the data (Sukumaran and Holder 2010), and (2) the coalescent-based species tree approach
124 ASTRAL III (Zhang et al. 2018).

125 ***Genetic diversity estimates.*** We estimated per-individual genetic diversity as the
126 observed heterozygosity across all genotyped sites (both variant and invariant). We estimated
127 ROH (runs of homozygosity) per individual across 25 kbp windows with no heterozygosity and
128 at least 80% of sites genotyped (i.e., 20+ kbp sites genotyped in 25 kbp windows).

129 ***Polymorphic TEs.*** We found ten endogenous retroviruses (ERVs) with more than 500
130 copies exhibiting low divergence from TE consensus sequences (Table S2). We used these ERVs
131 as candidates to look for between sample TE insertion polymorphisms with the Mobile Element
132 Locator Tool v2.1.2 (MELT; Gardner et al. 2017). MELT uses split and unaligned reads from the
133 BWA alignments, the reference genome, and consensus ERV sequences to identify polymorphic
134 ERVs. We used MELT in a multistep process: (1) discovery of potential ERVs per individual,
135 (2) grouping together putative polymorphic ERVs based on reference genome location, (3)
136 genotyping all individuals for the combined putative polymorphic ERV dataset, and (4) filtering

137 of all genotype calls. We ran these steps for each ERV separately, with a maximum 15%
138 divergence from the ERV consensus sequence. Any genomic coordinates (± 100 bp) called for
139 more than one ERV were filtered to the most similar ERV consensus sequence. We filtered the
140 final ERV polymorphisms by removing: (1) those with imprecise breakpoints or limited evidence
141 (MELT ASSESS flag ≥ 3), (2) polymorphisms not passing MELT's internal quality filters
142 (MELT FILTER flag \neq PASS), and (3) polymorphic ERVs with $> 25\%$ missing data.

143 **Demography.** We estimated demographic history for each individual using MSMC2
144 v1.1.0 (Schiffels and Durbin 2014). For use in MSMC, we masked genomic regions that were
145 not genotyped and sites with coverage of less than eight aligned reads (Nadachowska-Brzyska et
146 al. 2016). MSMC estimates are particularly accurate in panmictic populations, but population
147 structure or changes in gene flow between populations may mimic changes in population sizes
148 (Mazet et al. 2016; Chikhi et al. 2018). Therefore, some caution should be used when
149 interpreting raw demographic histories. However, we largely use the demographic histories to
150 estimate recent and harmonic mean population sizes and not strict interpretation of the
151 population trends. In MSMC, we allowed up to 20 iterations and up to 23 distinct time segments.
152 We performed ten bootstrap replicates (1 Mbp genomic segments) to assess how demographic
153 signal varied using different genomic regions. MSMC output is scaled relative to a species'
154 generation time and mutation rate. Here, we used double the age of sexual maturity as a
155 generation time proxy, as in previous studies (Nadachowska-Brzyska et al. 2015). Based on an
156 estimate of six months to sexual maturity (Moyle et al. 2009), we used a one-year generation
157 time. We used a mutation rate of 3.16×10^{-9} substitutions / site / year as reported from the *Z.*
158 *lateralis* genome (Cornetti et al. 2015).

159 **Island size estimation.** We manually measured the area of each island for all species in
160 the Solomon Islands using satellite imagery in Google Earth. For the one montane species, *Z.*
161 *murphyi*, we calculated the area of the species' range by calculating the area of the highland
162 region on the island of Kolombangara coincident with its estimated range.

163 **Statistical analysis.** We used R v4.4.1 (R Development Core Team 2023) to conduct an
164 array of statistical analyses. First, we visualized correlations among variables using a
165 correlogram made with corrplot v0.95 (Wei and Simko 2014). Second, we performed linear
166 regressions to examine the relationship between island size and our genetic variables. Third, due
167 to the high collinearity of the dataset, we performed LASSO regressions with GLMNET v4.1-8
168 (Friedman et al. 2010) to determine what variables were the most direct predictors of a given
169 response variable. Although island size is an explanatory variable, to determine how it impacted
170 different diversity metrics independently, we treated it as a response variable and all genomic
171 variables as predictors for a LASSO regression. LASSO regressions were performed with an
172 alpha value of 1 and lambda value selected by cross-validation.

173

174 **Results.**

175 We resequenced 17 *Zosterops* individuals from the Solomon Islands at 7–16x mean coverage
176 (Fig. S1; Table S1). Using 40,257 phylogenies, we identified a species tree consistent with
177 previous phylogenetic reconstructions using reduced-representation genomic methods (Fig. 1B;
178 Manthey et al. 2020).

179 **Demography.** Demographic history varied widely across *Zosterops* taxa in the Solomon
180 Islands (Fig. S2). Small island endemics generally have had small populations over the past
181 300,000 years (e.g., $N_E < 200,000$). Taxa with larger range sizes have experienced somewhat

182 fluctuating population sizes through time, and currently exhibit higher N_E than small island
183 endemics (e.g., N_E ranging 200,000 to 800,000). The demographic history of *Z. metcalfei* varies
184 widely by island and likely represents both changes in population sizes and population
185 connectivity with other island populations during Pleistocene glacial cycles. All *Z. metcalfei*
186 populations exhibited increases in population sizes prior to 100,000 years ago. Subsequently, the
187 population histories differed: (1) populations on the large islands of Choiseul and Isabel
188 experienced population declines 50,000 years ago followed by population size increases; (2) the
189 Shortland population has drastically declined in size in the last 50,000 years; (3) the Ngella
190 population has generally been smaller than on the larger islands, but more stable than Shortland.
191 Recent population sizes and harmonic mean population sizes over the past 200,000 years both
192 had a positive relationship with island size (Fig. 2A).

193 **Genomic Diversity.** Both genomic heterozygosity and variability in heterozygosity across
194 the genome varied widely. Individuals from smaller islands generally exhibited lower genomic
195 diversity and less variability (although not significantly, $p=0.056$) in diversity across the genome
196 relative to individuals on larger islands (Fig. 2C, 2D; Fig. S3; Table S1). Most metrics of genetic
197 diversity and effective population size covaried (Fig. S4). However, using a LASSO regression
198 treating island size as a response and these genomic metrics as predictors, only non-reference
199 ERVs, number of ROH, and recent population size were included in the final model (Table S3).

200 The number and total length of ROH were nearly perfectly correlated (Fig. S4, S5) and
201 higher in individuals from smaller islands (Fig. 2F). Notably, the *Z. luteirostris* individual from
202 Ghizo, the smallest island in our sample, showed the lowest genomic diversity and a highly
203 elevated amount of ROH (Fig. 2F). However, only the number and size of ROH on Ghizo were

204 both notable outliers relative to the other islands (Fig 2). When considering the number and
205 length of ROH segments, no islands strayed from a linear ratio of the two (Fig. S5).

206 ***TE Polymorphisms.*** We genotyped insertion presence/absence polymorphisms for ten
207 recently active ERVs. We identified ~3000 polymorphisms with 100 to 300 homozygous ERVs
208 absent in the reference genome per individual. Generally, individuals on smaller islands had
209 more homozygous non-reference ERVs than individuals on larger islands (Fig. 2D). The number
210 of homozygous non-reference ERVs was strongly, but not perfectly, correlated with
211 heterozygosity (Fig. S4). In a LASSO regression with non-reference ERVs as the response
212 variable, island size, heterozygosity, historic population size, and the total length of ROH
213 segments were included as predictors in the model (Table S3).

214

215 **Discussion.**

216 We demonstrated that island size is correlated with effective population size,
217 heterozygosity, and several other metrics related to genomic variability. Heterozygosity was not
218 the strongest correlate of island size, and LASSO regression with island size did not retain it as a
219 predictor, implying it did not explain sufficient unique variance relative to other variables (Table
220 S3). Instead, the LASSO regression recovered that island size was most directly correlated with
221 measures of recent population size, individual demography (i.e., ROH), and transposable element
222 activity. This reflects the myriad effects that population size can have on genomes. It is also
223 notable that these strong correlations arose from just modern island size, despite evidence of
224 gene flow within and among species. However, the legacy of gene flow facilitated by glacial
225 connectivity can still be seen in two medium-sized islands with high genetic diversity: Ngella
226 and Shortland. Both belong to the Pleistocene Bukida group, which ranged from Guadalcanal to

227 Shortland islands and included Bougainville (not sampled in this study). This group showed
228 elevated diversity compared to similarly sized islands (Fig. 2). However, they were not outliers
229 for recent effective population size, ROH metrics, and transposon activity, which we also found
230 as the most direct correlates of island size (Fig. 2, Table S3).

231 Runs of homozygosity (ROH) is one of the most important statistics in the modern
232 conservation genetics toolkit (Szpiech et al. 2013; Ceballos et al. 2018). This statistic is a
233 predictor of individual demography and inbreeding, and we found that island size is a predictor
234 of ROH (Fig. 2F). The small island of Ghizo has extremely high ROH statistics, despite not
235 being an outlier in any other metric (including overall genetic diversity). Additionally, its ratio
236 between sum of ROH lengths and number of ROH was consistent with other populations (Fig.
237 S5). Direct inbreeding (i.e., consanguineous individuals) is expected to produce fewer longer
238 ROH segments, while the observed pattern is consistent with a bottleneck or persistent low
239 population size (Ceballos et al. 2018). However, a bottleneck due to a founder effect is unlikely
240 in the deeply diverged *Z. luteirostris*, and persistent low population size should manifest itself in
241 other small New Georgia Group islands. Regardless, the high prevalence of ROH is a concern
242 for this species' genetic health, demonstrating the need for continued conservation attention
243 (Liligeto 2013). It is worth noting that the proportion of the genome contained within ROH is
244 low compared to other mammalian (Kyriazis et al. 2023; Bertola et al. 2024; Khan et al. 2024)
245 and avian (Martin et al. 2023) systems with small population sizes.

246 TEs are an important but not fully understood area of conservation genomics, as they are
247 often weakly deleterious and may diversify in small populations, where selective forces are
248 weaker (Jurka et al. 2011). Consistent with this hypothesis, we found that the number of
249 homozygous non-reference ERVs was correlated with island size. This could occur due to drift

250 (where ERVs act like neutral SNPs) and stronger selective forces against ERVs in larger
251 populations. Drift is likely a component of this phenomenon, but doesn't seem to be the only
252 one, as the negative correlation between homozygous ERVs and SNP heterozygosity is strong
253 but imperfect ($r = -0.83$), and both island size and genetic diversity were found to be predictors
254 in a LASSO model relating ERV fixation to other measured variables. Future work could further
255 explore whether ERV fixation is related to other metrics of natural selection, such as the
256 population-level synonymous and non-synonymous diversity ratio (Leroy et al. 2021).

257 Gene flow can be a major correlate of genetic diversity (Epps et al. 2005; Botigué et al.
258 2013), but we were not able to assess it directly in this study. However, Manthey et al. (2020)
259 recovered extensive gene flow among members of the Solomons *Zosterops* group, including two
260 sympatric taxa that lack current gene flow (Cowles and Uy 2019). One case of gene flow that
261 Manthey et al. (2020) recovered was between *Z. ugiensis* on Guadalcanal and *Z. metcalfi*. The
262 impact of this gene flow can be seen in the relatively low genetic diversity of the Makira—but
263 not Guadalacanal—population of this species. This finding is consistent with introgression from
264 *Z. metcalfi* into *Z. ugiensis*, thereby bolstering its genetic diversity. Such gene flow may help
265 explain why the correlation between genetic diversity and island size is not 1:1, as demonstrated
266 by the need to use the logarithm of island size as a predictor. That relationship could be
267 explained by Lewontin's paradox—the empirical finding that organisms show far lower genetic
268 diversity than would be expected based on census size (Lewontin 1974; Buffalo 2021)—and
269 density compensation—where smaller islands host fewer species at higher densities (MacArthur et
270 al. 1972; Wright 1980).

271 In sum, our results emphasize the strength of island size as a predictor of a wide range of
272 genomic variables. However, these variables are heavily correlated themselves, making it

273 difficult to untangle true relationships. Despite this shortcoming, we still recover unique signals
274 from different aspects of genomic diversity. Most importantly, we show that measuring multiple
275 metrics can reveal unique aspects of evolution, as we demonstrate here in this iconic geographic
276 radiation of white-eyes.

277 **Acknowledgements.**

278 We thank the Solomon Islands Ministry of Environment, Climate Change, Disaster Management,
279 and Meteorology for permits to conduct fieldwork (permit RP/2017/001) and the provincial
280 governments in the Solomon Islands that gave permission to conduct research. We are especially
281 indebted to the local communities that graciously invited us onto their lands and who provided
282 assistance and logistical support with field work. We thank D. Boseto and staff at Ecological
283 Solutions Solomon Islands for help with logistics, permitting, and fieldwork. We are grateful to
284 the University of Kansas Biodiversity Institute, American Museum of Natural History,
285 Smithsonian National Zoological Park, and University of Washington Burke Museum for
286 loaning tissues used in this study. This work was supported by National Science Foundation
287 grants (DEB-1557053 to RGM and DEB-1557051 to MJA) and startup from Texas Tech
288 University to JDM. We would also like to thank Manuel Hoyos for discussion about transposable
289 element evolution.

290

291 **Data, code and materials.**

292 All raw data is available on NCBI's sequence read archive (SRA) under BioProject ID:
293 PRJNA686795. All code to analyze the data is available
294 at github.com/jdmanthey/zosterops_genomes and archived on Dryad and Zenodo at
295 <https://doi.org/10.5061/dryad.z8w9ghxqf>.

296

297 **Figures and Tables.**

298 Figure 1. Sampling and phylogenomic relationships of *Zosterops* taxa used in this study. (A)

299 Sampling localities for this study. Dark gray indicates current island areas and lighter gray shows

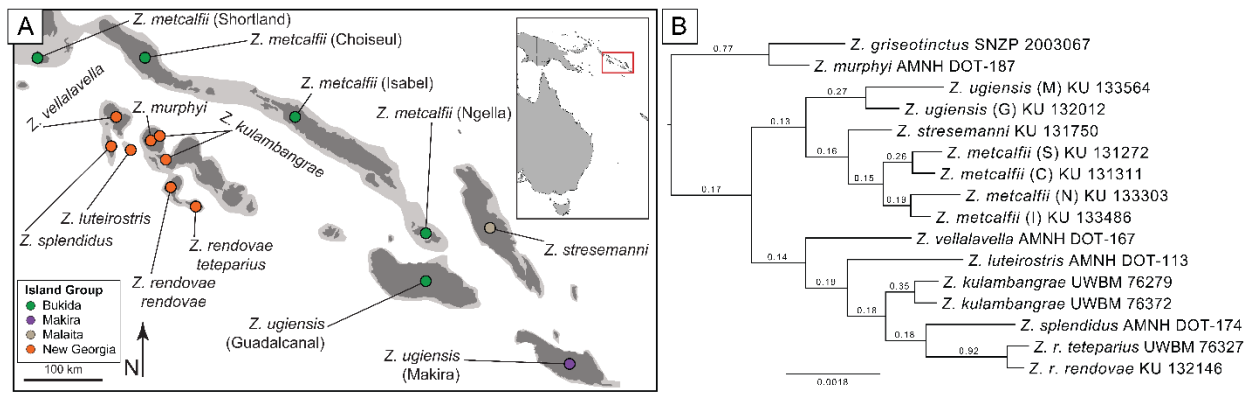
300 approximate land connectivity at low sea levels during Pleistocene glacial maxima. (B)

301 Maximum clade credibility tree from 40,257 phylogenies and rooted with *Z. simplex*. Numbers

302 above branches show the proportion of these phylogenies supporting specific relationships, and

303 all nodes had 100% support in the species tree with the same topology estimated in ASTRAL III.

304



305

306 Figure 2. Relationships of island size and genomic parameters. Island size is strongly correlated

307 with (A) recent and (B) harmonic mean of population size estimates in MSMC2, (C) genome-

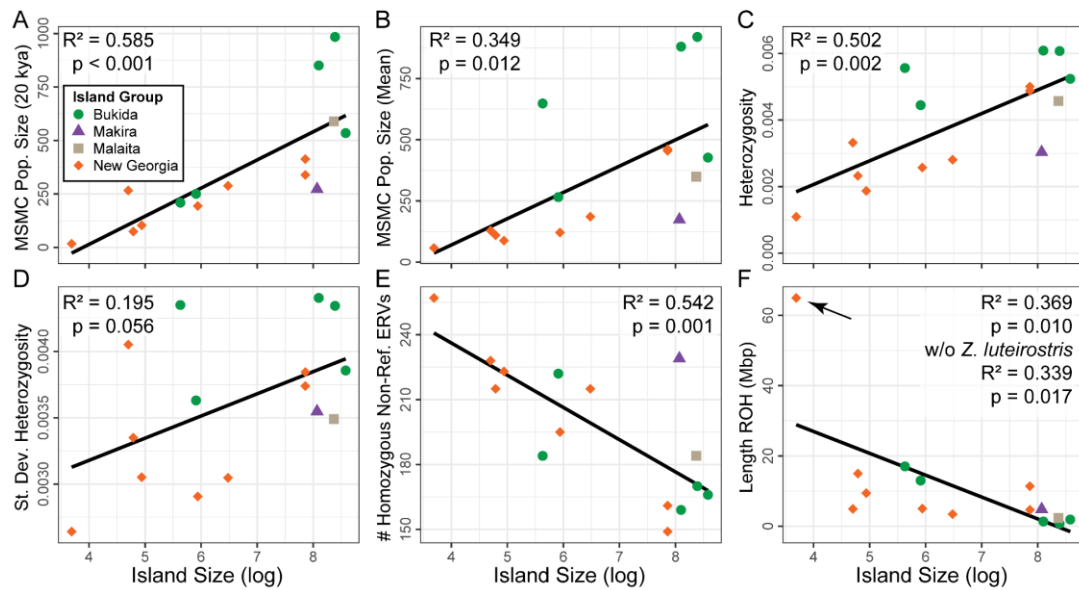
308 wide mean and (D) variability in heterozygosity, (E) homozygous non-reference endogenous

309 retroviruses (ERVs) and (F) total length of runs of homozygosity (ROH). In (F), regression was

310 performed with and without a putative outlier from the smallest island, but only the model with

311 the outlier is shown (denoted with an arrow). Point shape and color correspond to the island

312 group the population is from.



313

314

315 **References**

316 Bao Z., Eddy S.R. 2002. Automated de novo identification of repeat sequence families in
 317 sequenced genomes. *Genome Res.* 12:1269–1276.

318 Benson G. 1999. Tandem repeats finder: a program to analyze DNA sequences. *Nucleic Acids*
 319 *Res.* 27:573–580.

320 Bertola L.D., Quinn L., Hanghøj K., Garcia-Erill G., Rasmussen M.S., Balboa R.F., Meisner J.,
 321 Bøggild T., Wang X., Lin L., Nursyifa C., Liu X., Li Z., Chege M., Moodley Y., Brüniche-
 322 Olsen A., Kuja J., Schubert M., Agaba M., Santander C.G., Sinding M.-H.S., Muwanika V.,
 323 Masembe C., Siegismund H.R., Moltke I., Albrechtsen A., Heller R. 2024. Giraffe lineages
 324 are shaped by major ancient admixture events. *Curr. Biol.* 34:1576–1586.e5.

325 Botigué L.R., Henn B.M., Gravel S., Maples B.K., Gignoux C.R., Corona E., Atzmon G., Burns
 326 E., Ostrer H., Flores C., Bertranpetit J., Comas D., Bustamante C.D. 2013. Gene flow from

327 North Africa contributes to differential human genetic diversity in southern Europe. *Proc.*
328 *Natl. Acad. Sci. U. S. A.* 110:11791–11796.

329 Buffalo V. 2021. Quantifying the relationship between genetic diversity and population size
330 suggests natural selection cannot explain Lewontin’s Paradox. *Elife.* 10.

331 Bushnell B. 2014. BBMap: A fast, accurate, splice-aware aligner. .

332 Cai T., Cibois A., Alström P., Moyle R.G., Kennedy J.D., Shao S., Zhang R., Irestedt M.,
333 Ericson P.G.P., Gelang M., Qu Y., Lei F., Fjeldså J. 2018. Near-complete phylogeny and
334 taxonomic revision of the world’s babbler (Aves: Passeriformes). *Mol. Phylogenet. Evol.*

335 Camacho C., Coulouris G., Avagyan V., Ma N., Papadopoulos J., Bealer K., Madden T.L. 2009.
336 BLAST+: architecture and applications. *BMC Bioinformatics.* 10:421.

337 Ceballos F.C., Joshi P.K., Clark D.W., Ramsay M., Wilson J.F. 2018. Runs of homozygosity:
338 windows into population history and trait architecture. *Nat. Rev. Genet.* 19:220–234.

339 Chikhi L., Rodríguez W., Grusea S., Santos P., Boitard S., Mazet O. 2018. The IICR (inverse
340 instantaneous coalescence rate) as a summary of genomic diversity: insights into
341 demographic inference and model choice. *Heredity* . 120:13–24.

342 Cornetti L., Valente L.M., Dunning L.T., Quan X., Black R.A., Hébert O., Savolainen V. 2015.
343 The Genome of the “Great Speciator” Provides Insights into Bird Diversification. *Genome*
344 *Biol. Evol.* 7:2680–2691.

345 Costanzi J.-M., Steifetten Ø. 2019. Island biogeography theory explains the genetic diversity of a
346 fragmented rock ptarmigan (*Lagopus muta*) population. *Ecol. Evol.* 9:3837–3849.

347 Cowles S.A., Uy J.A.C. 2019. Rapid, complete reproductive isolation in two closely related
348 Zosterops White-eye bird species despite broadly overlapping ranges*. *Evolution*. 73:1647–
349 1662.

350 Cowles S.A., Weeks B.C., Perrin L., Chen N., Uy J.A.C. 2021. Comparison of adult census size
351 and effective population size support the need for continued protection of two Solomon
352 Island endemics. *Emu*. 121:45–54.

353 Danecek P., Auton A., Abecasis G., Albers C.A., Banks E., DePristo M.A., Handsaker R.E.,
354 Lunter G., Marth G.T., Sherry S.T., McVean G., Durbin R., 1000 Genomes Project Analysis
355 Group. 2011. The variant call format and VCFtools. *Bioinformatics*. 27:2156–2158.

356 Descimon H., Napolitano M. 1993. Enzyme polymorphism, wing pattern variability, and
357 geographical isolation in an endangered butterfly species. *Biol. Conserv.* 66:117–123.

358 Diamond J.M., Gilpin M.E., Mayr E. 1976. Species-distance relation for birds of the Solomon
359 Archipelago, and the paradox of the great speciators. *Proc. Natl. Acad. Sci. U. S. A.*
360 73:2160–2164.

361 Epps C.W., Palsbøll P.J., Wehausen J.D., Roderick G.K., Ramey R.R. II, McCullough D.R.
362 2005. Highways block gene flow and cause a rapid decline in genetic diversity of desert
363 bighorn sheep. *Ecol. Lett.* 8:1029–1038.

364 Frankham R. 1996. Relationship of genetic variation to population size in wildlife. *Conserv.*
365 *Biol.* 10:1500–1508.

366 Friedman J., Hastie T., Tibshirani R. 2010. Regularization paths for generalized linear models
367 via coordinate descent. *J. Stat. Softw.* 33:1–22.

368 Gardner E.J., Lam V.K., Harris D.N., Chuang N.T., Scott E.C., Pittard W.S., Mills R.E., 1000
369 Genomes Project Consortium, Devine S.E. 2017. The Mobile Element Locator Tool
370 (MELT): population-scale mobile element discovery and biology. *Genome Res.* 27:1916–
371 1929.

372 Gorman G.C., Soule M., Yang S.Y., Nevo E. 1975. Evolutionary Genetics of Insular Adriatic
373 Lizards. *Evolution.* 29:52.

374 Grabherr M.G., Russell P., Meyer M., Mauceli E., Alföldi J., Di Palma F., Lindblad-Toh K.
375 2010. Genome-wide synteny through highly sensitive sequence alignment: Satsuma.
376 *Bioinformatics.* 26:1145–1151.

377 Hill R., Loxterman J.L., Aho K. 2017. Insular biogeography and population genetics of dwarf
378 mistletoe (*Arceuthobium americanum*) in the Central Rocky Mountains. *Ecosphere.*
379 8:e01810.

380 Hoeck P.E.A., Bollmer J.L., Parker P.G., Keller L.F. 2010. Differentiation with drift: a spatio-
381 temporal genetic analysis of Galapagos mockingbird populations (*Mimus* spp.). *Philos.*
382 *Trans. R. Soc. Lond. B Biol. Sci.* 365:1127–1138.

383 Hughes A.R., Inouye B.D., Johnson M.T.J., Underwood N., Vellend M. 2008. Ecological
384 consequences of genetic diversity. *Ecol. Lett.* 11:609–623.

385 Jurka J., Bao W., Kojima K.K. 2011. Families of transposable elements, population structure and
386 the origin of species. *Biol. Direct.* 6:44.

387 Jurka J., Kapitonov V.V., Pavlicek A., Klonowski P., Kohany O., Walichiewicz J. 2005. Repbase
388 Update, a database of eukaryotic repetitive elements. *Cytogenet. Genome Res.* 110:462–

389 467.

390 Katoh K., Standley D.M. 2013. MAFFT multiple sequence alignment software version 7:
391 improvements in performance and usability. *Mol. Biol. Evol.* 30:772–780.

392 Khan A., Sil M., Thekaekara T., Garg K.M., Sinha I., Khurana R., Sukumar R., Ramakrishnan
393 U. 2024. Divergence and serial colonization shape genetic variation and define conservation
394 units in Asian elephants. *Curr. Biol.* 34:4692–4703.e5.

395 Kyriazis C.C., Beichman A.C., Brzeski K.E., Hoy S.R., Peterson R.O., Vucetich J.A., Vucetich
396 L.M., Lohmueller K.E., Wayne R.K. 2023. Genomic underpinnings of population
397 persistence in Isle Royale moose. *Mol. Biol. Evol.* 40.

398 Leroy, T., Rousselle, M., Tilak, M.-K., Caizergues, A. E., Scornavacca, C., Recuerda, M., Fuchs,
399 J., Illera, J. C., De Swardt, D. H., Blanco, G., Thébaud, C., Milá, B., Nabholz, B. 2021.
400 Island songbirds as windows into evolution in small populations. *Curr. Biol.* 31:1303–1310.

401 Lewontin R.C. 1974. Genetic basis of evolutionary change. New York, NY: Columbia
402 University Press.

403 Li H., Durbin R. 2009. Fast and accurate short read alignment with Burrows-Wheeler transform.
404 *Bioinformatics.* 25:1754–1760.

405 Li H., Handsaker B., Wysoker A., Fennell T., Ruan J., Homer N., Marth G., Abecasis G., Durbin
406 R., 1000 Genome Project Data Processing Subgroup. 2009. The Sequence Alignment/Map
407 format and SAMtools. *Bioinformatics.* 25:2078–2079.

408 Liligeto W. 2013. Gizo Environment Livelihood Conservation Association (GELCA) Resource

409 Management Plan. .

410 MacArthur R.H., Wilson E.O. 1963. An equilibrium theory of insular zoogeography. *Evolution*.
411 17:373–387.

412 MacArthur R.H., Wilson E.O. 1967. *The Theory of Island Biogeography*. Princeton, New Jersey:
413 Princeton University Press.

414 MacArthur, R. H., Diamond, J. M., & Karr, J. R. (1972). Density compensation in island faunas.
415 *Ecology*, 53(2), 330-342.

416

417 Manthey J.D., Oliveros C.H., Andersen M.J., Filardi C.E., Moyle R.G. 2020. Gene flow and
418 rapid differentiation characterize a rapid insular radiation in the southwest Pacific (Aves:
419 Zosterops). *Evolution*. 74:1788–1803.

420 Martin C.A., Sheppard E.C., Illera J.C., Suh A., Nadachowska-Brzyska K., Spurgin L.G.,
421 Richardson D.S. 2023. Runs of homozygosity reveal past bottlenecks and contemporary
422 inbreeding across diverging populations of an island-colonizing bird. *Mol. Ecol.* 32:1972–
423 1989.

424 Maurer B.A., Rosenzweig M.L. 1996. Species diversity in space and time. *Ecology*. 77:1314.

425 Mayr E. 1942. *Systematics and the Origin of Species*. New York: Columbia University Press.

426 Mazet O., Rodríguez W., Grusea S., Boitard S., Chikhi L. 2016. On the importance of being
427 structured: instantaneous coalescence rates and human evolution—lessons for ancestral
428 population size inference? *Heredity* . 116:362–371.

429 McKenna A., Hanna M., Banks E., Sivachenko A., Cibulskis K., Kernytsky A., Garimella K.,
430 Altshuler D., Gabriel S., Daly M., DePristo M.A. 2010. The Genome Analysis Toolkit: a
431 MapReduce framework for analyzing next-generation DNA sequencing data. *Genome Res.*
432 20:1297–1303.

433 Moyle R.G., Filardi C.E., Smith C.E., Diamond J.M. 2009. Explosive Pleistocene diversification
434 and hemispheric expansion of a “great speciator.” *Proc. Natl. Acad. Sci. U. S. A.* 106:1863–
435 1868.

436 Nadachowska-Brzyska K., Burri R., Smeds L., Ellegren H. 2016. PSMC analysis of effective
437 population sizes in molecular ecology and its application to black-and-white *Ficedula*
438 flycatchers. *Mol. Ecol.* 25:1058–1072.

439 Nadachowska-Brzyska K., Li C., Smeds L., Zhang G., Ellegren H. 2015. Temporal Dynamics of
440 Avian Populations during Pleistocene Revealed by Whole-Genome Sequences. *Curr. Biol.*
441 25:1375–1380.

442 Neall V.E., Trewick S.A. 2008. The age and origin of the Pacific islands: a geological overview.
443 *Philos. Trans. R. Soc. Lond. B Biol. Sci.* 363:3293–3308.

444 Oliveros C.H., Andersen M.J., Moyle R.G. 2021. A phylogeny of white-eyes based on
445 ultraconserved elements. *Mol. Phylogenet. Evol.* 164:107273.

446 Patton J.L. 1984. Genetical processes in the Galapagos. *Biol. J. Linn. Soc. Lond.* 21:97–111.

447 Preston F.W. 1962a. The Canonical Distribution of Commonness and Rarity: Part I. *Ecology.*
448 43:185.

449 Preston F.W. 1962b. The Canonical Distribution of Commonness and Rarity: Part II. *Ecology*.
450 43:410–432.

451 Price A.L., Jones N.C., Pevzner P.A. 2005. De novo identification of repeat families in large
452 genomes. *Bioinformatics*. 21 Suppl 1:i351–8.

453 Quinlan A.R., Hall I.M. 2010. BEDTools: a flexible suite of utilities for comparing genomic
454 features. *Bioinformatics*. 26:841–842.

455 R Development Core Team. 2023. R: A language and environment for statistical computing.
456 Vienna, Austria: R Foundation for Statistical Computing.

457 Sato J.J., Tasaka Y., Tasaka R., Gunji K., Yamamoto Y., Takada Y., Uematsu Y., Sakai E.,
458 Tateishi T., Yamaguchi Y. 2017. Effects of Isolation by Continental Islands in the Seto
459 Inland Sea, Japan, on Genetic Diversity of the Large Japanese Field Mouse, *Apodemus*
460 *speciosus* (Rodentia: Muridae), Inferred from the Mitochondrial Dloop Region. *Zoolog. Sci.*
461 34:112–121.

462 Schiffels S., Durbin R. 2014. Inferring human population size and separation history from
463 multiple genome sequences. *Nat. Genet.* 46:919–925.

464 Smit A.F.A., Hubley R. 2008. RepeatModeler Open-1.0. .

465 Smit A.F.A., Hubley R., Green P. 2015. RepeatMasker Open-4.0. 2013--2015. .

466 Soulé M.E. 1976. Allozyme variation, its determinants in space and time. In: Ayala F.J., editor.
467 *Molecular Evolution*. Sinauer Associates. p. 60–77.

468 Soulé M., Yang S.Y. 1973. GENETIC VARIATION IN SIDE-BLOTCHED LIZARDS ON

469 ISLANDS IN THE GULF OF CALIFORNIA. *Evolution*. 27:593–600.

470 Stamatakis A. 2014. RAxML version 8: a tool for phylogenetic analysis and post-analysis of
471 large phylogenies. *Bioinformatics*. 30:1312–1313.

472 Sukumaran J., Holder M.T. 2010. DendroPy: a Python library for phylogenetic computing.
473 *Bioinformatics*. 26:1569–1571.

474 Szpiech Z.A., Xu J., Pemberton T.J., Peng W., Zöllner S., Rosenberg N.A., Li J.Z. 2013. Long
475 runs of homozygosity are enriched for deleterious variation. *Am. J. Hum. Genet.* 93:90–102.

476 Tan D.J.X., Gyllenhaal E.F., Andersen M.J. 2023. PleistoDist: A toolbox for visualising and
477 quantifying the effects of Pleistocene sea-level change on island archipelagos. *Methods*
478 *Ecol. Evol.* 14:496–504.

479 Vinciguerra N.T., Oliveros C.H., Moyle R.G., Andersen M.J. 2023. Island life accelerates
480 geographic radiation in the white-eyes (*Zosteropidae*). *Ibis (Lond. 1859)*. 165:817–828.

481 Wang S., Zhu W., Gao X., Li X., Yan S., Liu X., Yang J., Gao Z., Li Y. 2014. Population size
482 and time since island isolation determine genetic diversity loss in insular frog populations.
483 *Molecular Ecology*. 23:637–648.

484 Warren W.C., Clayton D.F., Ellegren H., Arnold A.P., Hillier L.W., Künstner A., Searle S.,
485 White S., Vilella A.J., Fairley S., Heger A., Kong L., Ponting C.P., Jarvis E.D., Mello C.V.,
486 Minx P., Lovell P., Velho T.A.F., Ferris M., Balakrishnan C.N., Sinha S., Blatti C., London
487 S.E., Li Y., Lin Y.-C., George J., Sweedler J., Southey B., Gunaratne P., Watson M., Nam
488 K., Backström N., Smeds L., Nabholz B., Itoh Y., Whitney O., Pfenning A.R., Howard J.,
489 Völker M., Skinner B.M., Griffin D.K., Ye L., McLaren W.M., Flicek P., Quesada V.,

490 Velasco G., Lopez-Otin C., Puente X.S., Olender T., Lancet D., Smit A.F.A., Hubley R.,
491 Konkel M.K., Walker J.A., Batzer M.A., Gu W., Pollock D.D., Chen L., Cheng Z., Eichler
492 E.E., Stapley J., Slate J., Ekblom R., Birkhead T., Burke T., Burt D., Scharff C., Adam I.,
493 Richard H., Sultan M., Soldatov A., Lehrach H., Edwards S.V., Yang S.-P., Li X., Graves
494 T., Fulton L., Nelson J., Chinwalla A., Hou S., Mardis E.R., Wilson R.K. 2010. The genome
495 of a songbird. *Nature*. 464:757–762.

496 Wei T., Simko V. 2014. R package “corrplot”: Visualization of a Correlation Matrix (Version
497 0.95). .

498 Whittaker R.J., Fernández-Palacios J.M., Matthews T.J., Borregaard M.K., Triantis K.A. 2017.
499 Island biogeography: Taking the long view of nature’s laboratories. *Science*. 357:eaam8326.

500 Wright, S. J. (1980). Density compensation in island avifaunas. *Oecologia*, 45, 385-389.

501 Wright S. 1982. Character change, speciation, and the higher taxa. *Evolution*. 36:427–443.

502 Zhang C., Rabiee M., Sayyari E., Mirarab S. 2018. ASTRAL-III: polynomial time species tree
503 reconstruction from partially resolved gene trees. *BMC Bioinformatics*. 19.